Applied Surface Science 490 (2019) 365–371

Contents lists available at ScienceDirect

Applied Surface Science

journal homepage: www.elsevier.com/locate/apsusc

Full length article

Effect of Fe promotion on the performance of V_2O_5/MgF_2 catalysts for gas-phase dehydrofluorination of 1,1,1,3,3-pentafluoropropane

Xiu-Xiu Fang[a], Wen-Min Liao[a], Jian-Dong Song[a], Wen-Zhi Jia[b], Yun Wang[a], Ji-Qing Lu[a,*], Meng-Fei Luo[a,*]

[a] Key Laboratory of the Ministry of Education for Advanced Catalysis Materials, Institute of Physical Chemistry, Zhejiang Normal University, Jinhua 321004, China
[b] School of Chemistry and Chemical Engineering, Hubei Polytechnic University, Huangshi, Hubei 435003, China

ARTICLE INFO

Keywords:
Dehydrofluorination
HFC-245fa
3V-xFe/MgF_2
Fe promotion
Surface acidity

ABSTRACT

A series of 3V-xFe/MgF_2 catalysts with different V/Fe molar ratios were prepared by a sol-gel method, and the effect of Fe promotion on the catalytic performance of gas-phase dehydrofluorination of 1,1,1,3,3-pentafluoropropane (HFC-245fa) was investigated. It was found that proper V/Fe ratio was helpful to improve the activity. The 3V-0.5Fe/MgF_2 catalyst (with a V/Fe ratio of 6/1) gave a HFC-245fa conversion of 76.6% at 320 °C, which was 13.4% higher than that on the 3V/MgF_2 (63.2%). The synergy between V and Fe species resulted in enhanced surface acidity which accounts for the enhanced activity. The VO_x and FeO_x species in the fresh catalyst could be transformed to VOF_x and FeF_3 species during the reaction, which were regarded as the active sites. However, higher content of Fe in the catalyst resulted in the partial coverage of V species, which led to decline of surface acidity and thus the suppressed activity. Also, surface carbon deposition was responsible for the slight catalyst deactivation.

1. Introduction

As alternatives of chlorofluorocarbons (CFCs), hydrofluorocarbons (HFCs) such as 1,1,1,2-tetrafluoroethane (HFC-134a) are widely used as refrigerants, fire extinguishers, foaming agents, industrial solvents and detergents in modern society due to their zero ozone – depletion - potential (ODP) [1]. However, most of HFCs with high global warming potential (GWP) will be prohibited according to the Kyoto Protocol [2]. Hydrofluoroolefins (HFOs) are considered as an appealing substitution of HFCs because of their special properties such as short atmospheric life time, zero ODP and low GWP [3]. Among these HFO compounds, 1,3,3,3-tetrafluoropropene (HFO-1234ze), especially trans-1,3,3,3-tetrafluoropropene (HFO-1234ze (E)) has high refrigeration efficiency, good compatibility and with a very low GWP of 6, which is thus regarded as a potential candidate to more environmentally benign new generation fluorocarbons [4,5].

Recent years, it has been reported that HFO-1234ze can be efficiently synthesized via gas-phase dehydrofluorination of 1,1,1,3,3-pentafluoropropane (HFC-245fa), which is very promising because this reaction consumes HFC-245fa with high GWP (GWP = 858) [6–10]. In catalytic reaction involving HF and elevated temperature conditions (such as dehydrofluorination and chlorine/fluorine exchange reaction), metal fluorides and metal oxides such as AlF_3, MgF_2 and Cr_2O_3, Al_2O_3, MgO have been used as catalysts and/or supports owing to their irreplaceable stability under corrosive atmosphere [11–14]. For HFC dehydrofluorination, it is recognized that catalytic activity is related to the surface acidity of catalyst [15,16]. As a result, AlF_3 and fluorinated CrO_x (F-Cr_2O_3) are preferred catalysts owing to their strong surface acidity. For example, it was reported by Teinz et al. [17] that the dehydrofluorination of 3-chloro-1,1,1,3-tetrafluorobutane took place on the strong Lewis acid sites in the AlF_3 catalyst. Besides, Han et al. [18] disclosed that Cr_2O_3 nanoparticles prepared by a solution combustion method showed 2-fold higher activity in the dehydrofluorination of 1,1-difluoroethane to produce vinyl fluoride owing to the higher surface acidity on the former catalyst. Recently, Han et al. [19] found that the Cr/Al composite catalysts fabricated via simple solution combustion method with high Lewis acidic sites dramatically facilitate the dehydrofluorination of HFC-152a. Although AlF_3 and F-Cr_2O_3 are active catalysts in the dehydrofluorination reactions, fast deactivation is often observed in these catalysts due to severe coke deposition on the strong acid sites. For these reasons, the design and fabrication of new catalyst materials is an urgent need for the preparation of HFOs by dehydrofluorination reactions in commercial processes, and yet it remains very challenging.

* Corresponding authors.
E-mail addresses: jiqinglu@zjnu.cn (J.-Q. Lu), mengfeiluo@zjnu.cn (M.-F. Luo).

https://doi.org/10.1016/j.apsusc.2019.06.103
Received 3 May 2019; Received in revised form 9 June 2019; Accepted 11 June 2019
Available online 13 June 2019
0169-4332/

Magnesium fluoride (MgF_2), characteristic of good thermal stability and weak acid centers, make it an excellent support for various transition metal oxides [20,21]. Song et al. [6] found that the addition of V_2O_5 in MgF_2 resulted in up to 5-fold increase in HFC-245fa conversion (from 19.2 to 95.2% at 340 °C) and much enhanced catalyst stability due to the MgF_2 support triggered the transformation of V_2O_5 to vanadium oxyfluoride (VOF_x) species via the reaction between V_2O_5 and HF. Very recently, Jia et al. [7] has investigated the catalytic behaviors of a series of hollow nano-MgF_2 supported catalysts (M/nano-MgF_2, M = Al^{3+},Cr^{3+}, Fe^{3+}, Co^{3+}, Zn^{2+} and Ni^{2+}), and found that the 9% Al/nano-MgF_2 was more active than the traditional AlF_3 and F-Cr_2O_3 for gas phase dehydrofluorination of HFC-245fa.

It is well known that additives may improve the catalytic performance of catalysts through changing redox and/or acid properties [22–25]. Feng et al. [26] reported that the catalytic performance of the V and Fe incorporated HMS in the hydroxylation of benzene with hydrogen peroxide as the oxidant was related to the V/Fe ratios and the addition of Fe creates new acid sites and a stronger redox ability. Tanarungsun et al. [27] reported that phenol yield increased from 1.2% over Fe/TiO_2 to 7.3% over the FeVCu/TiO_2 catalyst using H_2O_2 as the oxidant and found that the increase of activity was related to the enhancement of catalyst acidity.

In current work, the role of Fe as a promoter for the 3V-xFe/MgF_2 catalysts for gas-phase dehydrofluorination of 1,1,1,3,3-pentafluoropropane is investigated. The influences of catalyst components such as the molar ratio of V/Fe on the catalyst structures and catalytic performance have been studied. This study aimed to provide a general method to prepare highly effective catalysts for the dehydrofluorination reaction. It is found that the addition of Fe in the catalysts not only affects the oxidation states of the V species but also the surface acidity of the catalysts, which consequently exerts great influences on their catalytic behaviors.

2. Experimental

2.1. Catalyst preparation

MgF_2 catalyst was prepared by directly mixing $Mg(NO_3)_2{\cdot}6H_2O$ (analytical grade, Shanghai Aladdin Biochemical Technology Co., Ltd.) aqueous solution and NH_4F (analytical grade, Tianjin kwangfu Fine Chemical Industry Research Institute) aqueous solution with a Mg^{2+}: F^- molar ratio of 1:2, stirred for 10 min, aged at room temperature for 4 h, dried at 100 °C overnight, and then calcined in air at 400 °C for 4 h with a ramp of 10 °C min^{-1}.

The 3V-xFe/MgF_2 catalysts were prepared by a sol-gel method. Taking the 3V-0.5Fe/MgF_2 catalyst (the V molar percentage per mole MgF_2 was 3%, the Fe molar percentage per mole MgF_2 was 0.5%) as an example, a detailed process was as follows. 8.2315 g $Mg(NO_3)_2{\cdot}6H_2O$ (32.10 mmol), 2.3782 g NH_4F (64.20 mmol), 0.1161 g NH_4VO_3 (0.99 mmol, analytical grade, Shanghai Macklin Biochemical Technology Co., Ltd.), 0.0650 g $Fe(NO_3)_3{\cdot}9H_2O$ (0.16 mmol, analytical grade, Sinopharm Group Chemical Reagent Co., Ltd.) and 3 ml deionized water were mixed and stirred for 10 min at room temperature until a reddish yellow sol was obtained. After the sol was aged at room temperature for 4 h, the excess water was evaporated at 90 °C and the solid was dried at 100 °C overnight. Finally, the resulting solid was calcined at 400 °C for 4 h with a ramp of 10 °C min^{-1} in static air to obtain the catalyst, which was denoted as 3V-0.5Fe/MgF_2. Other 3V-xFe/MgF_2 catalysts with different Fe contents and the reference Fe/MgF_2 catalyst were also prepared in a similar manner. The V molar percentage per mole MgF_2 was kept at 3%, while the Fe molar percentages per mole MgF_2 ranged from 0.3 to 2%, which were denoted as 3V-0.3Fe/MgF_2, 3V-0.5Fe/MgF_2, 3V-1Fe/MgF_2 and 3V-2Fe/MgF_2. The reference catalyst with Fe only (Fe molar percentages per mole MgF_2 was 3%) was denoted as 3Fe/MgF_2.

2.2. Catalyst characterizations

Powder X-ray diffraction (XRD) patterns were measured on a Bruker D8 ADVANCE powder diffractometer with a Cu Kα radiation (λ = 0.15418 nm) in a 2θ range from 10 to 90°, with an operating voltage of 40 kV and an operating current of 40 mA. Surface areas of the catalysts were determined by N_2 adsorption isotherms at 77 K on a NOVA 4000e apparatus. Before the measurements, the samples were outgassed at 200 °C for 4 h under vacuum.

The Raman spectra were recorded under ambient conditions using a Renishaw Invia reflex Raman spectrometer under ambient condition (laser power = 3 mW, dwell time = 60 s, number of scans = 4, resolution = 1 cm^{-1}). The wavelength of the excitation laser was 325 nm and the scanning range was 100–2000 cm^{-1}.

X-ray photoelectron spectra (XPS) of the catalysts were measured on an ESCALAB 250Xi instrument, with an Al Kα X-ray source (1486.6 eV). The binding energies were calibrated using F1 s speak at 685.5 eV as a reference.

Temperature-programmed desorption of ammonia (NH_3-TPD) experiments were conducted to measure the surface acidity of the catalysts. About 80 mg of the sample was placed in a Micromeritics AutoChem II 2920 instrument and pretreated in pure He at 300 °C for 30 min, then it was cooled down to 50 °C and exposed to anhydrous ammonia gas (10% in He) for 30 min. Weakly adsorbed NH_3 was purged by a He flow (30 ml min^{-1}) treatment at the same temperature for 30 min. Then the sample was heated in the He flow from 50 to 800 °C at a rate of 20 °C min^{-1}, and the profile was recorded by a thermal conductivity detector (TCD).

Surface acidity of the catalyst was further determined by in situ Fourier transform infrared (FTIR) spectroscopy of pyridine adsorption, which was performed on a Bruker TENSOR 27 FTIR spectrometer. About 16 mg of the sample was pressed into a 13 mm self-supported wafer and placed into an in situ IR cell. The sample was then heated from room temperature to 350 °C at a rate of 10 °C min^{-1} under vacuum. The sample was kept at 350 °C for 2 h and then cooled to 150 °C, and the background spectrum was collected. The sample was further cooled down to room temperature and exposed to pyridine vapor for 10 min. Then it was purged at 150 °C for 30 min in a He flow, followed by the spectrum recording in the range of 1200–1700 cm^{-1} with 32 scans and at a resolution of 4 cm^{-1}.

2.3. Catalytic testing

Gas phase dehydrofluorination of HFC-245fa was carried out in a stainless-steel tubular reactor (10 mm (i.d.) × 300 mm) under atmospheric pressure. 0.4 g of the catalyst (40–60 mesh, with a volume of about 0.4 ml) was loaded into the reactor with a thermal couple placed in the middle of the catalyst bed to monitor the reaction temperature. The catalyst was pretreated in a N_2 flow (30 ml min^{-1}) at 300 °C for 30 min. Then the N_2 flow was switched to a mixture of N_2 and HFC-245fa with a flow ratio of HFC-245fa / N_2 = 3.2/10.8 ml min^{-1} was introduced (total flow = 14 ml min^{-1}, GHSV = 2100 h^{-1}). To remove the product HF, the reaction effluent passed an aqueous KOH solution and then it was analyzed by a gas chromatograph (Shimadzu GC-2014) equipped with a flame ionization detector (FID) and a GS-GASPRO capillary column (0.32 mm × 60 m). Carbon balances were close to 100 ± 3%.

3. Results and discussion

3.1. Characterizations of 3V-xFe/MgF_2 catalysts

The XRD patterns of the fresh and spent 3V-xFe/MgF_2 catalysts (the spent catalysts refer to those after 4 h reaction) are shown in Fig. 1. As shown in Fig. 1a, the fresh 3V/MgF_2 shows distinct diffractions at 2θ of 27.2, 35.2, 40.0, 43.7, 53.5, 56.2, 60.7 and 68.1°, which are attributed

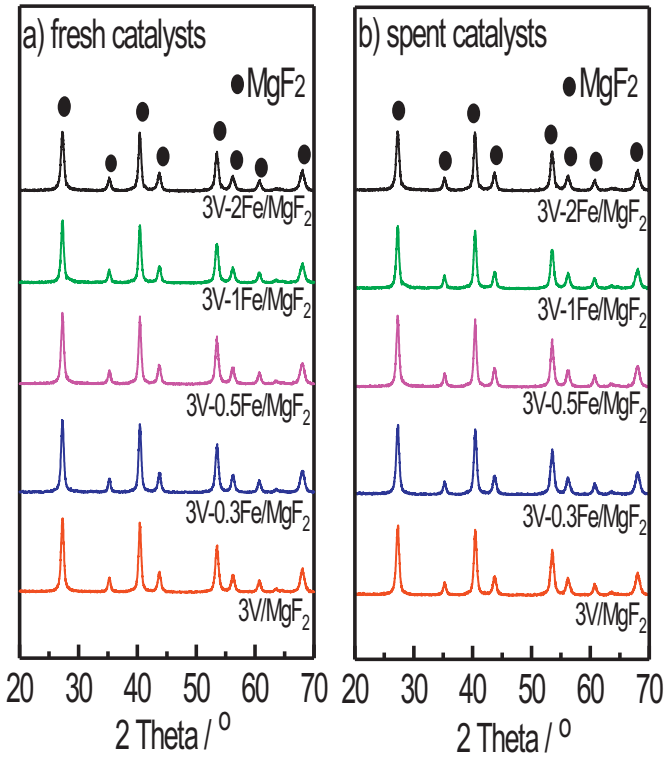

Fig. 1. XRD patterns of a) fresh and b) spent 3V-xFe/MgF_2 catalysts.

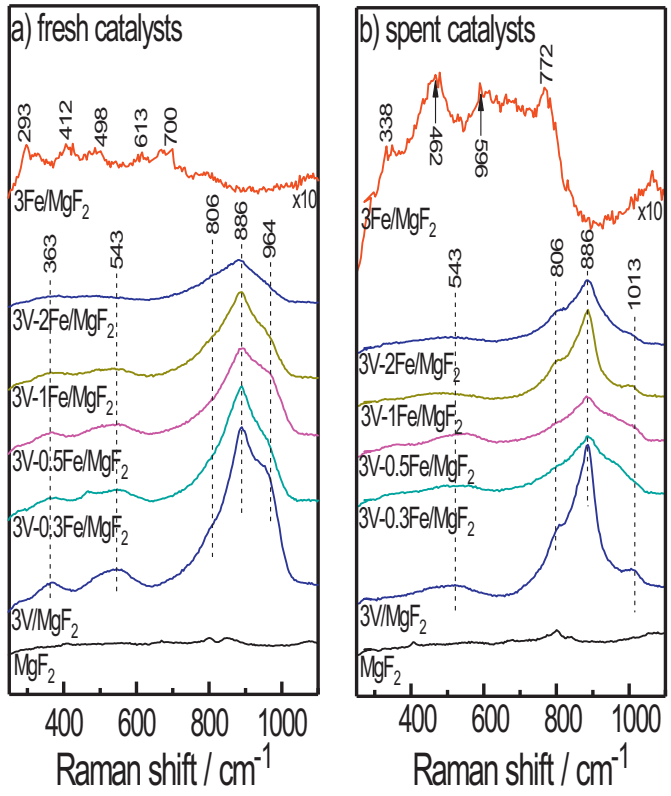

Fig. 2. Raman spectra of a) fresh and b) spent 3V-xFe/MgF_2 catalysts.

to crystalline MgF_2 (JCPDS No. 41-1443). No diffractions related to vanadium species are observed, indicating that these species are highly dispersed on the support. The addition of FeO_x in the 3V/MgF_2 catalyst does not alter the crystalline structure as the patterns of the Fe-containing samples are identical to that of the 3V/MgF_2 and no diffraction of FeO_x species are detected. The absence of the diffraction related to iron species suggests the high dispersion of such species on the support due to the low loadings. For the spent catalysts (Fig. 1b), it is found that the diffractions are identical to those of the corresponding fresh ones, implying that the crystalline structures of the catalysts hardly change during the reaction process.

Raman spectroscopy is a powerful tool to determine the surface species. Fig. 2 shows the Raman spectra of the fresh and spent 3V-xFe/MgF_2 catalysts. For the fresh catalysts (Fig. 2a), the MgF_2 support merely shows any Raman bands. The amplified spectrum of the 3Fe/MgF_2 sample shows several weak bands at 293, 412, 498, 613 and 700 cm^{-1} related to Fe_2O_3 [28,29]. The V-containing catalysts show two weak bands at 363 and 543 cm^{-1}, three large and overlapped bands centered at 806, 886 and 964 cm^{-1}. The bands at 363 and 543 cm^{-1} are attributed to $\delta_{V\text{-}O}$ (363 cm^{-1}) and $\delta_{V=O}$ (543 cm^{-1}), which are attributed to typical bond vibrations of polymeric VO_x [30,31]. The bands at 806, 886 and 964 cm^{-1} are attributed to V-O-V and V=O stretching modes in polyvanadate species, respectively [32]. Moreover, the intensities of the bands related to vanadium species gradually decrease with increasing Fe content in the catalyst, which may be due to the decreasing crystallinity of V_2O_5, i.e. the increase of disorder. For the spent catalysts (Fig. 2b), the MgF_2 support does not show any bands. The spent 3Fe/MgF_2 did not show bands characteristic of Fe_2O_3 (bands at 293, 412, 498, 613 and 700 cm^{-1}), instead, four new weak bands at 338, 462, 596 and 772 cm^{-1} emerge, which could be assigned to FeF_3 [33]. The transformation of the iron species after reaction suggests that the FeO_x could react with the fluorine-containing compounds (either the reactant HFC-245fa or HFO-1234ze and HF produced in the reaction). For the spent V-containing samples, the bands at 363, 543 and 964 cm^{-1} disappear but the bands at 806 and 886 cm^{-1} remains, and a new weak band at 1013 cm^{-1} is observed. These findings suggest that vanadium oxide in the catalyst could be transformed to some new surface species. Such species have also been observed in our previous work [6] on V_2O_5/MgF_2 catalysts prepared by an impregnation method, which is a strong indication of the formation of VOF_x species via the reaction between VOx and HFO-1234ze or HF.

Fig. 3 shows the V 2p XPS spectra of the fresh and spent 3V-xFe/MgF_2 catalysts. The V $2p_{3/2}$ peak of the fresh 3V-xFe/MgF_2 catalysts (Fig. 3a) could be resolved to two components at binding energies (BEs) of 516.3 and 517.2 eV, which could be assigned to V^{3+} and V^{5+}, respectively [34]. The generation of V^{3+} species is likely due to the reduction of surface V_2O_5 under the XPS experiment conditions such as high vacuum and X-ray radiation [34] or due to the V—Fe interaction. Also, one interesting observation is that the concentration of surface V^{3+} species gradually increases with increasing FeO_x contents in the catalyst while that of the surface V^{5+} species decreases (Table 1), which clearly indicates the presence of V—Fe interaction and the presence of FeO_x species is helpful to stabilize the V^{3+} species in the catalyst. Unfortunately, the analysis of Fe XPS spectra is not successful because the Fe 2p spectrum overlaps with that of the Mg 1 s and the Fe 3 s spectrum overlaps with that of the F 1 s. For the spent 3V-xFe/MgF_2 catalysts (Fig. 3b), two components at BEs of 517.3 and 518.3 eV are observed. The component at BE of 517.3 eV is assigned to V^{5+} species in the catalyst, while that at BE of 518.3 eV is assigned to V species with much lowered electron density. Such withdraw of electron from V atom is reported to be related to the formation of VOF_x species, in which the F atoms is much more electronegative and thus extract electron from vanadium to fluorine [6]. This observation again indicates the formation of new V species during the reaction, due to the reaction between vanadium oxides (most likely V^{3+}) and fluorine-containing compounds (i.e. HF or HFO-1234ze). However, part of the VO_x species remain intact during the reaction, which is also evidenced by the Raman spectroscopic results (Fig. 2) as the band at 886 cm^{-1} still exists in all the catalysts. It also implies that the vanadium species in form of

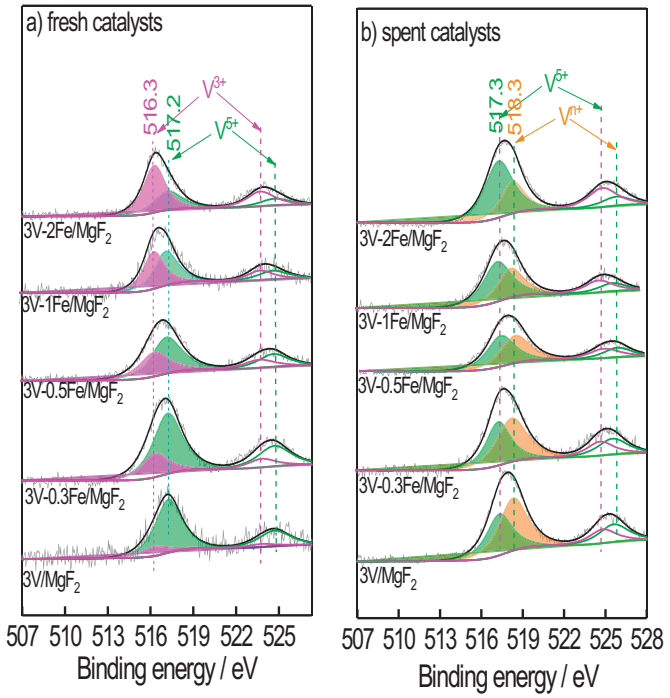

Fig. 3. XPS spectra of a) fresh and b) spent 3V-xFe/MgF_2 catalysts.

Table 1
Surface concentration of V^{3+} and V^{5+} species in various fresh and spent 3V-xFe/MgF_2 catalysts based on XPS analysis.

Catalyst	Fresh catalysts		Spent catalysts	
	V^{3+} (%)	V^{5+} (%)	V^{5+} (%)	V^{n+} in VOF_x (%)
3V/MgF_2	14.8	85.2	42.0	58.0
3V-0.3Fe/MgF_2	26.3	73.7	44.8	55.2
3V-0.5Fe/MgF_2	38.9	61.6	51.9	48.1
3V-1Fe/MgF_2	48.4	51.6	60.0	40.0
3V-2Fe/MgF_2	65.0	35.0	68.4	31.6

polyvanadate are stable in the fluorine-containing environment while those highly dispersed monovanadate could be transformed to VOF_x. Table 1 also shows that the surface concentration of VOF_x (V^{n+}) in the spent catalyst decreases with increasing Fe content. This might be due to the partial coverage of VO_x by FeO_x during the preparation process upon increasing FeO_x content, thus hindering the formation of such VOF_x species.

Fig. 4 shows the NH_3-TPD profiles of three representative catalysts to illustrate the changes of their surface acidity before and after reaction. All the catalysts (either fresh and spent ones) show broad NH_3 desorption peaks in temperature range of 100–550 °C, suggesting the presence of weak (100–200 °C), medium (200–400 °C) and strong (400–550 °C) acid sites in the catalysts. As for the fresh catalysts, the 3V/MgF_2 has a surface acidity of 16.2 μmol g^{-1}, which is lower than those of the 3V-0.5Fe/MgF_2 (28.5 μmol g^{-1}). However, the 3V-2Fe/MgF_2 has lower acidity (12.1 μmol g^{-1}) than that of the 3V/MgF_2. This observation indicates that the addition of small quantity of Fe in the catalyst could enhance the surface acidity due to the Fe—V interaction. However, excessive Fe species may cover the vanadium sites and thus suppress the surface acidity. Compared to the corresponding fresh ones, the spent catalysts give much enhanced surface acidity. For example, the spent 3V-0.5Fe/MgF_2 has higher surface acidity (40.7 μmol g^{-1}) than the fresh one. Such enhanced surface acidity further implies the formation of new surface species which are more acidic than the vanadium oxide and iron oxide. Indeed, the presence of VOF_x species

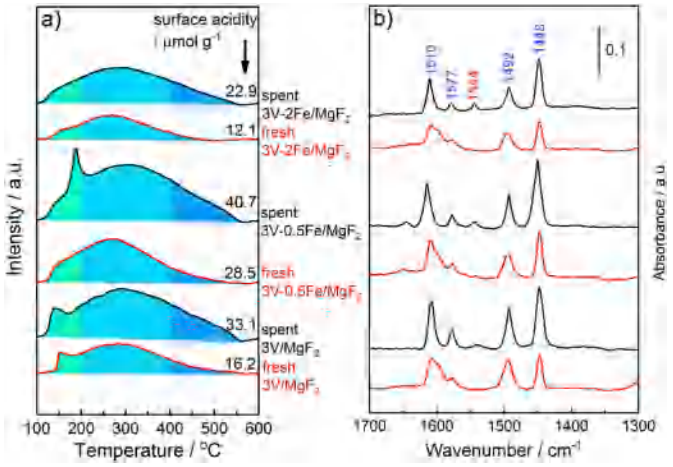

Fig. 4. a) NH_3-TPD profiles and b) pyridine - FTIR of fresh and spent 3V/MgF_2, 3V-0.5Fe/MgF_2 and 3V-2Fe/MgF_2 catalysts.

(evidenced by the XPS results, Fig. 3b) and FeF_3 species (evidenced by the Raman results, Fig. 2b) in the spent catalysts would certainly enhance the surface acidity as the F atoms in these species attract electrons from V and Fe. Fig. 4b demonstrates the FTIR spectra of pyridine adsorption on the catalysts. All the measured catalysts show four feature bands at 1448, 1492, 1577 and 1610 cm^{-1}, which indicates the presence of Lewis acid sites [35,36]. In addition, the band intensities of the fresh catalysts follow an order of 3V-2Fe/MgF_2 < 3V/MgF_2 < 3V-0.5Fe/MgF_2, which is consistent with the NH_3-TPD results (Fig. 4a). For the spent catalysts, it is found that a very weak band at 1545 cm^{-1} assigning to Brønsted acid site is observed [37], implying the formation of such acid sites during the reaction process. However, the quantity of the Brønsted acid site is rather limited. Moreover, compared to the corresponding fresh catalyst, the band intensities of the spent one is higher, indicating the enhanced surface acidity due to the formation of new surface species which possess higher acidity.

3.2. Catalytic performance of 3V-xFe/MgF_2 catalysts

Fig. 5 shows the catalytic performance of the 3V-xFe/MgF_2 catalysts for dehydrofluorination of HFC-245fa at different reaction temperatures. All the catalysts give a rising HFC-245fa conversion at the elevated reaction temperature, and the conversions are closed to 100% when the reaction temperature is up to 400 °C, which is consistent with the description in literature [38] that the synthesis of HFO-1234ze by dehydrofluorination of HFC-245fa was an endothermic reaction, and the change of standard Gibbs free energy declined with the increasing reaction temperature. The MgF_2 is inactive at low temperatures (< 360 °C), with a HFC-245fa conversion of < 10%. The addition of 3 mol% of Fe in the MgF_2 slightly improves the activity. The 3V/MgF_2 catalyst gives a HFC-245fa conversion of 63.2% at 320 °C, which is higher than that on the 3Fe/MgF_2, indicating that the vanadium species is more active than the iron species. The co-addition of V and Fe improves the overall performance. For example, the 3V-0.3Fe/MgF_2 and 3V-0.5Fe/MgF_2 catalysts show higher conversions (69.5 and 77.6%, respectively) than the 3V/MgF_2 (63.2%) at 320 °C. However, higher contents of Fe in the catalyst (i.e. 1 and 2 wt%) result in a decline of overall activity (Table 2).

Table 2 summarizes the surface areas, HFC-245fa conversions, HFO-1234ze selectivities and E/Z ratio of various catalysts. The supported 3V-xFe/MgF_2 catalysts have slightly lower surface areas (34.5–41.7 $m^2 g^{-1}$) than the 3V/MgF_2 (43.5 $m^2 g^{-1}$). All the catalysts show almost 100% of selectivity to HFO-1234ze (the minor products are 3,3,3-trifluoropropyne and 2,3,3,3-tetrafluoropropene (HFO-1234yf)), with a trans- (E)/cis- (Z) ratio of 4. Specific reaction rates are

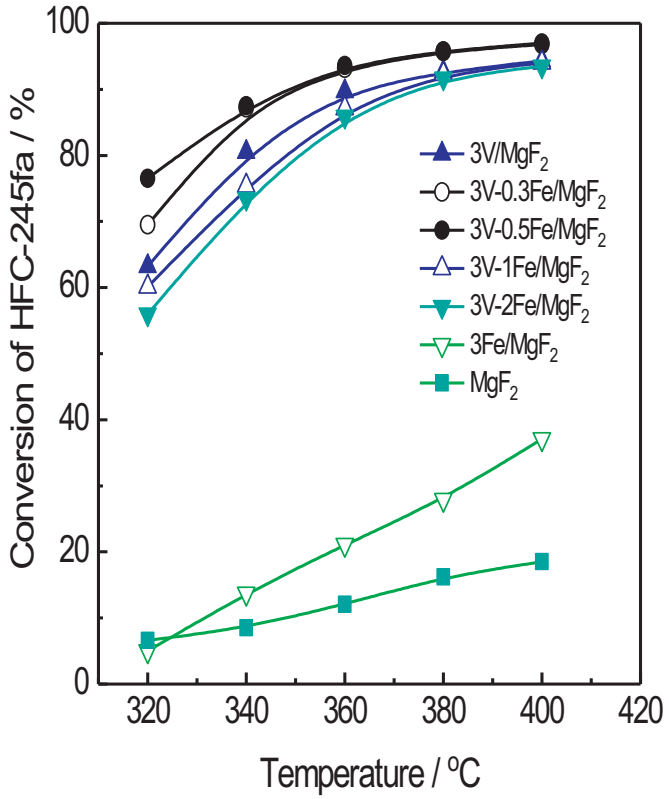

Fig. 5. HFC-245fa conversion on the 3V-xFe/MgF_2 catalysts at different reaction temperatures.

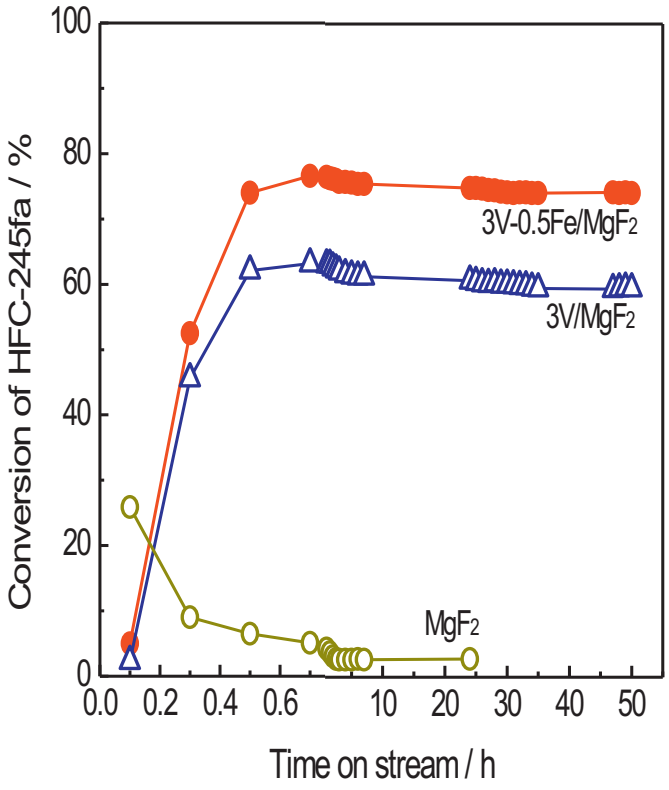

Fig. 6. Stability of MgF_2, 3V/MgF_2 and 3V-0.5Fe/MgF_2 catalysts at 320 °C.

also calculated in order to compare the catalytic performance with the catalysts reported in literature. At the reaction temperature of 320 °C, the V-0.5Fe/MgF_2 catalyst has the highest reaction rate (4.49 μmol s^{-1} $g_{cat}{}^{-1}$ and 0.111 μmol s^{-1} m^{-2}), which is higher than those reported on fluoride-based catalysts (i.e. 2.11 μmol s^{-1} $g_{cat}{}^{-1}$and 0.015 μmol s^{-1} m^{-2} over the AlF3-AOH catalyst [8]; 2.68 μmol s^{-1} $g_{cat}{}^{-1}$ and 0.067 μmol s^{-1} m^{-2} over the V_2O_5/MgF2 catalyst [6]) and is comparable to those reported on Cr-based catalyst (i.e. 11.6 μmol s^{-1} $g_{cat}{}^{-1}$, 0.335 μmol s^{-1} m^{-2} over the Cr2O3 catalyst and 16.8 μmol s^{-1} $g_{cat}{}^{-1}$, 0.093 μmol s^{-1} m^{-2} over the NiO/Cr2O3 catalyst [9]). Therefore, a small amount of Fe played a major role in the catalyst.

Fig. 6 demonstrates stability of the MgF_2, 3V/MgF_2 and 3V-0.5Fe/MgF_2 catalysts at reaction temperature of 320 °C. The HFC-245fa conversion on the MgF_2 support declines from 25.9 to 2.7% after 10 h reaction. In contrast, the conversion on the 3V/MgF_2 and 3V-0.5Fe/MgF_2 slightly declines from 63.2% and 76.6% at 1 h respectively to 59.5% and 74.9% at 50 h, suggesting that the stability of the catalyst is further improved by addition of Fe. Moreover, an apparent induction period is observed on the 3V/MgF_2 and 3V-0.5Fe/MgF_2 catalysts. The conversion increases rapidly in the first 30 min (from 2.3 to 62.1% and 3.2 to 74.5%, respectively), and then it reaches a steady state. Such induction period has been observed in our previous work on similar V/MgF_2 catalysts, which was attributed to the support-induced formation of active VOF_x species during the reaction [6] as evidenced by the Raman (Fig. 2) and XPS (Fig. 3) results in the current work.

It has been well documented in literature that the catalyst activity in dehydrofluorination reaction is closely related to its surface acidity because the crucial adsorption and the cleavage of C—F bond in the reactant molecule takes place on the surface acid site of the catalyst [15,19]. For example, an early work by Okazaki and coworkers reported dehydrofluorination of CF_3CH_3 over various metal fluorides catalysts [39], and it was found that AlF_3 catalyst with Lewis acid sites showed the highest activity. Very recently, Jia et al. [40] found that the weak and medium Lewis acid sites derived from NiF_2-AlF_3 complex phase are active centers for catalyzing dehydrofluorination of CF_3CH_2F to trifluoroethylene (CF_2 = CHF). In the current work, the catalysts (either fresh or spent) contain dominantly surface Lewis acid sites

Table 2
Surface areas, HFC-245fa conversions and HFO-1234ze selectivities on 3V-xFe/MgF_2 catalysts.

Catalyst	S_{BET} /m^2 g^{-1}	Conv.[a] /%	Reaction rate		Selectivity to HFO-1234ze /%		E/Z ratio
			/μmol s^{-1} $g_{cat}{}^{-1}$	/μmol s^{-1} m^{-2}	E	Z	
MgF_2	21.3	6.6	0.39	0.019	80.1	19.3	4.15
3V/MgF_2	43.5	63.2	3.71	0.085	80.5	19.1	4.21
3V-0.3Fe/MgF_2	41.7	69.5	4.41	0.106	81.1	18.4	4.41
3V-0.5Fe/MgF_2	40.5	76.6	4.49	0.111	81.3	18.2	4.47
3V-1Fe/MgF_2	37.5	60.1	3.58	0.095	81.0	18.4	4.40
3V-2Fe/MgF_2	34.5	56.1	3.34	0.097	79.8	18.7	4.26
3Fe/MgF_2	27.5	5.0	0.30	0.011	76.0	19.6	3.87

[a] Reaction temperature = 320 °C, data were taken after 1 h reaction.

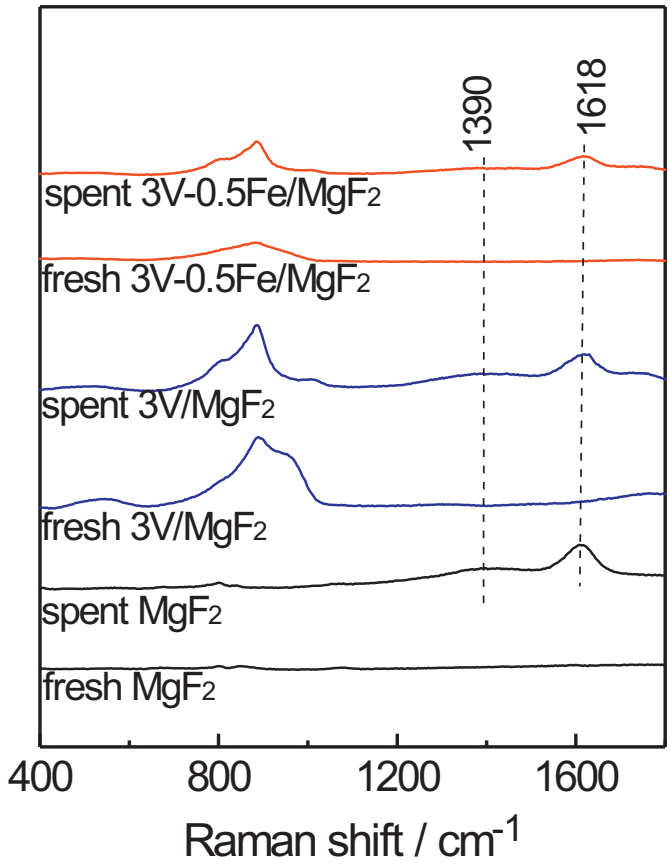

Fig. 7. Raman spectra of fresh and spent MgF_2, $3V/MgF_2$ and $V\text{-}0.5Fe/MgF_2$ catalysts.

(Fig. 4b), which further vindicates the roles of such acid sites in the dehydrofluorination reaction. Moreover, the surface acidity changes much from the fresh catalyst to the corresponding spent one (Fig. 4), which well explains the observation of the induction period due to the formation of new surface V and Fe species which are more acidic than the oxides. In addition, the overall activities of the representative $3V/MgF_2$, $3V\text{-}0.5Fe/MgF_2$ and $3V\text{-}2Fe/MgF_2$ catalysts follow an order of $3V\text{-}2Fe/MgF_2 < 3V/MgF_2 < 3V\text{-}0.5Fe/MgF_2$ (Table 2 and Fig. 5), which is consistent with trend of surface acidity (Fig. 4). Therefore, it is reasonable to reach the conclusion that the surface Lewis acid sites are the active sites for the reaction.

It is worthwhile to discuss the roles of Fe species in changing the catalyst properties and consequently the catalytic behaviors. The XPS results of the fresh catalysts with different Fe contents (Table 1 and Fig. 3) reveal that the interaction between V and Fe somehow reduces the average valence of the surface V species (higher concentration of V^{3+} in the Fe-containing catalysts). Such surface V^{3+} species could be transformed to active VOF_x species during the reaction. Meanwhile, the surface FeO_x species could also be transformed to FeF_3 as evidenced by the Raman spectra (Fig. 2). Moreover, the XPS analyses of the spent catalysts (Table 1 and Fig. 3b) reveal that too much FeF_3 species in the catalyst results in a decline of surface concentration of VOF_x, as the $3V\text{-}2Fe/MgF_2$ contains the lowest surface concentration of VOF_x (31.6%). Consequently, it results in decreased surface acidity and thus lowered activity.

We could further derive the intrinsic activities of VOF_x and FeF_3 species, based on the following equation:

$$\text{Overall rate} = \text{rate of } VOF_x \times C_{VOFx} + \text{rate of } FeF_3 \times C_{FeF3},$$

where overall rate is the reaction rates ($mol_{HFC\text{-}245fa}\ g_{cat}^{-1}\ s^{-1}$) of the catalysts at 320 °C which are listed in Table 2; rate of VOF_x and rate of FeF_3 are the specific reaction rates of VOF_x ($mol_{HFC\text{-}245fa}\ mol_{VOF}^{-1}\ s^{-1}$) and FeF_3 ($mol_{HFC\text{-}245fa}\ mol_{FeF3}^{-1}\ s^{-1}$); C_{VOFx} ($mol_{VOFx}\ g_{cat}^{-1}$) and C_{FeF3} ($mol_{FeF3}\ g_{cat}^{-1}$) are contents of surface VOF_x and FeF_3 species in the catalyst, respectively, which could be calculated based on the nominal contents of VO_x and FeO_x in the catalyst and the XPS results (Table 1, all the FeO_x species are assumed to be transformed to FeF_3). By multilinear regression of the data, the rate of VOF_x at 320 °C is calculated to be 1.53×10^{-2} $mol_{HFC\text{-}245fa}\ mol_{VOF}^{-1}\ s^{-1}$ ($TOF = 1.53 \times 10^{-2}\ s^{-1}$), and that of the FeF_3 is 0.95×10^{-2} $mol_{HFC\text{-}245fa}\ mol_{FeF3}^{-1}\ s^{-1}$ ($TOF = 0.95 \times 10^{-2}\ s^{-1}$). These results indicate that both the VOF_x and FeF_3 species are active sites for the reaction, but the VOF_x species are more active than the FeF_3 species.

Catalyst stability is very important in practical application. The catalysts employed in the current work are quite stable during 50 h reaction, however, slight deactivation is observed on the $3V/MgF_2$ and $3V\text{-}0.5Fe/MgF_2$ catalysts (Fig. 6). The catalyst deactivation has been extensively investigated in literature and it is due to the coke deposition on the catalyst surface because of the surface acidity [6,10]. For example, Li et al. [16] reported that carbon deposition and/or polymerization take place on strong acid sites in the $Mg_2P_2O_7$ catalyst for the dehydrofluorination of 1,1,1-trifluoroethane to 1,1-difluoroethylene. Our recent work [41] reported that pre-deposited carbonaceous species formed in the catalyst due to the incomplete decomposition of organic precursors during the preparation procedure, which blocked strong acidic sites in the AlF_3 and thus maintained the catalyst stability. Fig. 7 compares the Raman spectra of fresh and spent MgF_2, $3V/MgF_2$ and $3V\text{-}0.5Fe/MgF_2$ catalysts. It is clear that no Raman bands other than the surface VO_x species (in range of 400–1000 cm^{-1}) are detected on the fresh catalysts. However, new Raman bands at 1390 and 1618 cm^{-1} are observed on the spent catalysts, which are characteristics of carbon deposition [42,43]. Therefore, it could be concluded that the catalyst deactivation is due to the carbon deposition on the catalyst surface during the reaction. In addition, the bands intensities on the $3V\text{-}0.5Fe/MgF_2$ catalyst are much weaker than those on the MgF_2 and $3V/MgF_2$ catalysts, indicating that the addition of Fe in the $3V\text{-}xFe/MgF_2$ can inhibit the formation of carbon deposit because of the decrease of strong acidity on catalyst surface, thus keeping the catalyst more stable.

4. Conclusions

This work presents a study of dehydrofluorination over supported $3V\text{-}xFe/MgF_2$ catalysts. It is found that the addition of Fe in the $3V\text{-}xFe/MgF_2$ enhances both activity and stability. The incorporation of Fe and V with proper molar ratio could improve the catalytic performance. The VO_x and FeO_x in the fresh catalysts could be transformed to VOF_x and FeF_3 species during the reaction, which are believed to be the active sites. It is also found that the VOF_x is more active than the FeF_3, and high content of Fe in the catalyst results in decline of surface acidity and consequently the decline of activity. Besides, surface carbon deposition is detected on the spent catalysts, which accounts for the slight catalyst deactivation.

Acknowledgment

This work was financially supported by the National Natural Science Foundation of China (No. 21603069 and 21872124).

References

[1] Z.T. Liu, L. Liu, J. Wu, J. Lu, P. Sun, L.P. Song, Z.W. Liu, W.S. Dong, Z.W. Gao, Ind. Eng. Chem. Res. 46 (2007) 22–28.
[2] G.J. Velders, D.W. Fahey, J.S. Daniel, M. McFarland, S.O. Andersen, Proc. Nat. Acad. Sci. 106 (2009) 10949–10954.
[3] M.K. Vollmer, S. Reimann, M. Hill, D. Brunner, Environ. Sci. Technol. 49 (2015) 2703–2708.
[4] A. Mota-Babiloni, J. Navarro-Esbrí, F. Molés, Á.B. Cervera, B. Peris, G. Verdú, Appl.

Therm. Eng. 95 (2016) 211–222.
[5] Z. Yang, X. Wu, T. Tian, Energy 91 (2015) 386–392.
[6] J.D. Song, T.Y. Song, T.T. Zhang, Y. Wang, M.F. Luo, J.Q. Lu, J. Catal. 364 (2018) 271–281.
[7] Z.H. Jia, W. Mao, Y.B. Bai, B. Wang, H. Ma, C. Li, J. Lu, Appl. Catal. B Environ. 238 (2018) 599–608.
[8] W. Mao, Y.B. Bai, Z.H. Jia, Z.Q. Yang, Z.J. Hao, J. Lu, Appl. Catal. A-Gen 564 (2018) 147–156.
[9] J.W. Luo, J.D. Song, W.Z. Jia, Z.Y. Pu, J.Q. Lu, M.F. Luo, Appl. Surf. Sci. 433 (2018) 904–913.
[10] F. Wang, W.X. Zhang, Y. Liang, Y. Wang, J.Q. Lu, M.F. Luo, Chem. Res. Chin. Univ. 31 (2015) 1003–1006.
[11] E. Kemnitz, Catal. Sci. Technol. 5 (2015) 786–806.
[12] E. Kemnitz, Y. Zhu, B. Adamczyk, J. Fluor. Chem. 114 (2002) 163–170.
[13] D.H. Cho, Y.G. Kima, M.J. Chung, J.S. Chung, Appl. Catal. B Environ. 18 (1998) 251–261.
[14] Y. Zhu, K. Fiedler, St. Rüdiger, E. Kemnitz, J.Catal. 219 (2003) 8–16.
[15] W.Z. Jia, M. Liu, X.W. Lang, C. Hu, J.H. Li, Z.R. Zhu, Catal. Sci. Technol. 5 (2015) 3103–3107.
[16] G.L. Li, H. Nishiguchi, T. Ishihara, Y. Moro-Oka, Y. Takita, Appl. Catal. B Environ. 16 (1998) 309–317.
[17] K. Teinz, S. Wuttke, F. Börno, J. Eicher, E. Kemnitz, J. Catal. 282 (2011) 175–182.
[18] W.F. Han, Z.K. Wang, X.J. Li, H.D. Tang, M. Xi, Y. Li, H.Z. Liu, J. Mater. Sci. 51 (2016) 11002–11013.
[19] W.F. Han, B. L, X.L. Li, L.T. Yang, J.C. Wang, H.D. Tang, W.C. Liu, Ind. Eng. Chem. Res. 57 (2018) 12774–12783.
[20] M. Wojciechowska, M. Zieliński, M. Pietrowski, J. Fluor. Chem. 120 (2003) 1–11.
[21] M. Wojciechowska, W. Gut, M. Grunwald-Wyspian'ska, Catal. Lett. 15 (1992) 237–245.
[22] X.X. Wang, H.Y. Zheng, X.J. Liu, G.Q. Xie, J.Q. Lu, L.Y. Jin, M.F. Luo, Appl. Catal. A-Gen 388 (2010) 134–140.
[23] A. Huidobro, A. Sep'ulveda-Escribano, F. Rodr'ıguez-Reinoso, J. Catal.. 212 (2002) 94–103.
[24] A. Sirijaruphan, J.G. Goodwin Jr., R.W. Rice, J. Catal. 224 (2004) 304–313.
[25] D.I. Jerdev, A. Olivas, B.E. Koel, J. Catal. 205 (2002) 278–288.
[26] S.J. Feng, B. Yue, Y. Wang, Y. Lin, H.Y. He, Acta Phys. -Chim. Sin. 27 (2011) 2881–2886.
[27] G. Tanarungsun, W. Kiatkittipong, P. Praserthdam, H. Yamada, T. Tagawa, S.J. Assabumrungrat, Ind. Eng. Chem. 14 (2008) 596–601.
[28] R.J. Thibeau, C.W. Brown, R.H. Heidersbach, Appl. Spectrosc. 32 (1978) 532.
[29] D.L.A. de Faria, S. Venaüncio Silva, M.T. de Oliveira, J. Raman Spectrosc. 28 (1997) 873–878.
[30] A. Khodakov, B. Olthof, A.T. Bell, E. Iglesia, J. Catal. 181 (1999) 205–216.
[31] C. Sanchez, J. Livage, G. Lucazeau, J. Raman Spectrosc. 12 (1982) 68–72.
[32] M. Harlin, V. Niemi, A. Krause, J. Catal. 195 (2000) 67–78.
[33] A.E. Meixner, R.E. Dietz, D.L. Rousseau, Phys. Rev.B 7 (1973) 3134–3141.
[34] C. Hess, G. Tzolova-Müller, R. Herbert, J. Phys. Chem. C 111 (2007) 9471–9479.
[35] H. Choi, J.H. Bae, D.H. Kim, Y.K. Park, J.K. Jeon, Materials 6 (2013) 1718–1729.
[36] H. Lee, H.D. Jeong, Y.S. Chung, G.L. Han, M.J. Chung, S. Kim, H.S. Kim, J. Catal. 169 (1997) 307–316.
[37] M.V. Martínez-Huerta, X. Gao, H. Tian, I.E. Wachs, J.L.G. Fierro, M.A. Bañares, Catal. Today 118 (2006) 279–287.
[38] J.W. Luo, Y. Liang, W.X. Zhang, B.T. Teng, Y.J. Wang, M.F. Luo, Org. Fluor. Ind. 2 (2015) 1–6.
[39] S. Okazaki, S. Toyota, Nikkashi, (1972), pp. 1615–1617.
[40] W.Z. Jia, Y.F. Chen, M. Liu, X. Liu, X.H. Liu, J.J. Yuan, X.J. Lua, Z.R. Zhu, Appl. Catal. A-Gen 571 (2019) 150–157.
[41] X.X. Fang, Y. Wang, W.Z. Jia, J.D. Song, Y.J. Wang, M.F. Luo, J.Q. Lu, Appl. Catal. A-Gen 576 (2019) 39–46.
[42] C.A. Johnson, K.M. Thomas, Fuel 63 (1984) 1073–1080.
[43] C. Casiraghi, F. Piazza, A.C. Ferrari, D. Gramboleb, J. Robertsona, Diam. Relat. Mater. 14 (2005) 1098–1102.